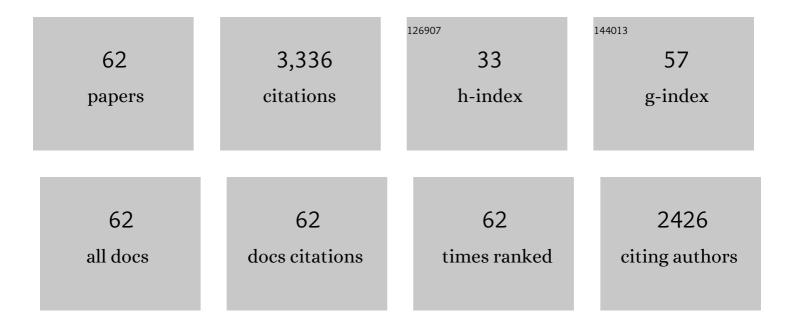
Hyeong-Ki Kim

List of Publications by Year in descending order

Source: https://exaly.com/author-pdf/3505029/publications.pdf Version: 2024-02-01



#	Article	IF	CITATIONS
1	Self-healing of Portland and slag cement binder systems incorporating circulating fluidized bed combustion bottom ash. Construction and Building Materials, 2022, 314, 125571.	7.2	7
2	Coal bottom ash. , 2022, , 29-60.		3
3	Electrical resistivity stability of CNT/cement composites after further hydration: A simple evaluation with an accelerated method. Construction and Building Materials, 2022, 317, 125830.	7.2	7
4	Effect of chloride penetration on electrical resistivity of CNT–CF/cement composites and its application as chloride sensor for reinforced mortar. Cement and Concrete Composites, 2022, 133, 104662.	10.7	8
5	Effects of crumb rubber particles on mechanical properties and sustainability of ultra-high-ductile slag-based composites. Construction and Building Materials, 2021, 272, 121959.	7.2	23
6	Structural Performance and Reinforcement Improvement of Structural Walls Using Strain-Hardening Cementitious Composites. Sustainability, 2021, 13, 3607.	3.2	1
7	Flowability and electrical properties of cement composites with mechanical dispersion of carbon nanotube. Construction and Building Materials, 2021, 293, 123436.	7.2	19
8	A Study on Mechanical Characteristics of Cement Composites Fabricated with Nano-Silica and Carbon Nanotube. Applied Sciences (Switzerland), 2021, 11, 152.	2.5	7
9	Deep-Learning-Based Segmentation of Fresh or Young Concrete Sections from Images of Construction Sites. Materials, 2021, 14, 6311.	2.9	4
10	Practical considerations of porosity, strength, and acoustic absorption of structural pervious concrete. Case Studies in Construction Materials, 2021, 15, e00764.	1.7	6
11	Examining the potential of calcined oyster shell waste as additive in high volume slag cement. Construction and Building Materials, 2020, 230, 116973.	7.2	38
12	Use of circulating fluidized bed combustion bottom ash as a secondary activator in high-volume slag cement. Construction and Building Materials, 2020, 234, 117240.	7.2	22
13	Utilization of controlled low strength material (CLSM) as a novel grout for geothermal systems: Laboratory and field experiments. Journal of Building Engineering, 2020, 29, 101110.	3.4	10
14	Evaluation of time to shrinkage-induced crack initiation in OPC and slag cement matrices incorporating circulating fluidized bed combustion bottom ash. Construction and Building Materials, 2020, 257, 119507.	7.2	16
15	Mechanical and Fiber-Bridging Behavior of Slag-Based Composite with High Tensile Ductility. Applied Sciences (Switzerland), 2020, 10, 4300.	2.5	6
16	On the expansive cracking of a cement matrix containing atomized basic oxygen furnace slag with a metallic iron. Construction and Building Materials, 2020, 264, 119806.	7.2	8
17	Parametric modeling of autogenous shrinkage of sodium silicate-activated slag. Construction and Building Materials, 2020, 262, 120747.	7.2	10
18	On the quantification of degrees of reaction and hydration of sodium silicate-activated slag cements. Materials and Structures/Materiaux Et Constructions, 2020, 53, 1.	3.1	6

Ηγεονς-Κι Κιμ

#	Article	IF	CITATIONS
19	Hydration kinetics modeling of sodium silicate-activated slag: A comparative study. Construction and Building Materials, 2020, 242, 118144.	7.2	17
20	Effects of the type of activator on the self-healing ability of fiber-reinforced alkali-activated slag-based composites at an early age. Construction and Building Materials, 2019, 224, 980-994.	7.2	24
21	Chloride-induced corrosion of steel fiber near the surface of ultra-high performance concrete and its effect on flexural behavior with various thickness. Construction and Building Materials, 2019, 224, 206-213.	7.2	62
22	Effect of Carbonation on Abrasion Resistance of Alkali-Activated Slag with Various Activators. Materials, 2019, 12, 2812.	2.9	4
23	Mechanical properties and self-healing capacity of eco-friendly ultra-high ductile fiber-reinforced slag-based composites. Composite Structures, 2019, 229, 111401.	5.8	21
24	Incorporation of CFBC ash in sodium silicate-activated slag system: Modification of microstructures and its effect on shrinkage. Cement and Concrete Research, 2019, 123, 105771.	11.0	19
25	Fluctuation of electrical properties of carbon-based nanomaterials/cement composites: Case studies and parametric modeling. Cement and Concrete Composites, 2019, 102, 55-70.	10.7	23
26	The role of carbon nanotube on hydration kinetics and shrinkage of cement composite. Composites Part B: Engineering, 2019, 169, 55-64.	12.0	63
27	Effects of quartz-based mine tailings on characteristics and leaching behavior of ultra-high performance concrete. Construction and Building Materials, 2018, 166, 110-117.	7.2	62
28	Utilization of by-product in controlled low-strength material for geothermal systems: Engineering performances, environmental impact, and cost analysis. Journal of Cleaner Production, 2018, 172, 909-920.	9.3	36
29	Internal curing effect of raw and carbonated recycled aggregate on the properties of high-strength slag-cement mortar. Construction and Building Materials, 2018, 165, 64-71.	7.2	40
30	Abrasion resistance of ultra high performance concrete incorporating coarser aggregate. Construction and Building Materials, 2018, 165, 11-16.	7.2	62
31	Utilization of circulating fluidized bed combustion ash in producing controlled low-strength materials with cement or sodium carbonate as activator. Construction and Building Materials, 2018, 159, 642-651.	7.2	44
32	Use of recycled aggregates as internal curing agent for alkali-activated slag system. Construction and Building Materials, 2018, 159, 286-296.	7.2	56
33	Effects of a defoamer on the compressive strength and tensile behavior of alkali-activated slag-based cementless composite reinforced by polyethylene fiber. Composite Structures, 2017, 172, 166-172.	5.8	50
34	Flexural stress and crack sensing capabilities of MWNT/cement composites. Composite Structures, 2017, 175, 86-100.	5.8	67
35	Fresh and hardened properties of ultra-high performance concrete incorporating coal bottom ash and slag powder. Construction and Building Materials, 2017, 131, 459-466.	7.2	124
36	Effect of chloride content on mechanical properties of ultra high performance concrete. Cement and Concrete Composites, 2017, 84, 175-187.	10.7	61

Нуеонд-Кі Кім

#	Article	IF	CITATIONS
37	Effects of coarser fine aggregate on tensile properties of ultra high performance concrete. Cement and Concrete Composites, 2017, 84, 28-35.	10.7	74
38	Carbon nanotube/cement composites for crack monitoring of concrete structures. Composite Structures, 2017, 180, 741-750.	5.8	60
39	Effect of fiber addition on fresh and hardened properties of spun cast concrete. Construction and Building Materials, 2016, 125, 306-315.	7.2	2
40	Utilization of excavated soil in coal ash-based controlled low strength material (CLSM). Construction and Building Materials, 2016, 124, 598-605.	7.2	59
41	Recycling of arsenic-rich mine tailings in controlled low-strength materials. Journal of Cleaner Production, 2016, 118, 151-161.	9.3	38
42	Heating and heat-dependent mechanical characteristics of CNT-embedded cementitious composites. Composite Structures, 2016, 136, 162-170.	5.8	110
43	Effects of Crushed Coal Bottom Ash on the Properties of Mortar with Various Water-to-binder Ratios. Journal of the Korean Institute of Resources Recycling, 2016, 25, 29-40.	0.4	0
44	Utilization of sieved and ground coal bottom ash powders as a coarse binder in high-strength mortar to improve workability. Construction and Building Materials, 2015, 91, 57-64.	7.2	97
45	Coal bottom ash in field of civil engineering: A review of advanced applications and environmental considerations. KSCE Journal of Civil Engineering, 2015, 19, 1802-1818.	1.9	83
46	Chloride penetration monitoring in reinforced concrete structure using carbon nanotube/cement composite. Construction and Building Materials, 2015, 96, 29-36.	7.2	60
47	Feasibility study on measurement of water absorption in fine aggregate with macroporous surface via centrifugal compaction. Construction and Building Materials, 2015, 95, 421-430.	7.2	4
48	Properties of Normal-Strength Mortar Containing Coarsely-Crushed Bottom Ash Considering Standard Particle Size Distribution of Fine Aggregate. Journal of the Korea Concrete Institute, 2015, 27, 531-539.	0.2	5
49	Enhanced effect of carbon nanotube on mechanical and electrical properties of cement composites by incorporation of silica fume. Composite Structures, 2014, 107, 60-69.	5.8	280
50	Improved chloride resistance of high-strength concrete amended with coal bottom ash for internal curing. Construction and Building Materials, 2014, 71, 334-343.	7.2	57
51	Improved piezoresistive sensitivity and stability of CNT/cement mortar composites with low water–binder ratio. Composite Structures, 2014, 116, 713-719.	5.8	178
52	Mechanical and Chemical Characteristics of Bottom Ash Aggregates Cold-bonded with Fly Ash. Journal of the Korean Ceramic Society, 2014, 51, 57-63.	2.3	5
53	Alkali-activated, cementless, controlled low-strength materials (CLSM) utilizing industrial by-products. Construction and Building Materials, 2013, 49, 738-746.	7.2	73
54	Microbially mediated calcium carbonate precipitation on normal and lightweight concrete. Construction and Building Materials, 2013, 38, 1073-1082.	7.2	120

Ηγεονς-Κι Κιμ

#	Article	IF	CITATIONS
55	Flow, water absorption, and mechanical characteristics of normal- and high-strength mortar incorporating fine bottom ash aggregates. Construction and Building Materials, 2012, 26, 249-256.	7.2	75
56	Workability, and mechanical, acoustic and thermal properties of lightweight aggregate concrete with a high volume of entrained air. Construction and Building Materials, 2012, 29, 193-200.	7.2	235
57	Influence of silica fume additions on electromagnetic interference shielding effectiveness of multi-walled carbon nanotube/cement composites. Construction and Building Materials, 2012, 30, 480-487.	7.2	109
58	Use of power plant bottom ash as fine and coarse aggregates in high-strength concrete. Construction and Building Materials, 2011, 25, 1115-1122.	7.2	204
59	Electromagnetic interference shielding characteristics and shielding effectiveness of polyaniline-coated films. Thin Solid Films, 2011, 519, 3492-3496.	1.8	103
60	Influence of cement flow and aggregate type on the mechanical and acoustic characteristics of porous concrete. Applied Acoustics, 2010, 71, 607-615.	3.3	119
61	Acoustic absorption modeling of porous concrete considering the gradation and shape of aggregates and void ratio. Journal of Sound and Vibration, 2010, 329, 866-879.	3.9	77
62	Utilization of power plant bottom ash as aggregates in fiber-reinforced cellular concrete. Waste Management, 2010, 30, 274-284.	7.4	73